Paper published in Applied Acoustics 170 (2020) 107536 [accepted 13/7/20]
DOI: 10.1016/ j.apacoust.2020.107536

The influence of track design on the rolling noise from trams

Wenjing Sun[1], David Thompson[2], Martin Toward[2], Marcus Wiseman[2], Evangelos Ntotsios[2], Stephen Byrne[3]

[1] Institute of Rail Transit, Tongji University, Shanghai 201804, P.R. China

[2] Institute of Sound and Vibration Research, University of Southampton, Southampton SO17 1BJ, United Kingdom

[3] Transport Infrastructure Ireland, Dublin, Republic of Ireland

Abstract: Tramway noise can be significant even though the speeds are relatively low. The influence of track design on the rolling noise is studied through a systematic comparison of different tracks on a single network. These include a slab track with embedded sleeper blocks, a ballasted track and a track with embedded rails. Measurements have been taken of rail vibration and noise during tram passages at approximately 55 km/h; the rail and wheel roughness have also been measured. Comparisons are made in terms of track decay rate, rail vibration and pass-by noise. After normalising to the same roughness, the slab track is found to be the noisiest and the ballasted track the quietest. Theoretical models of the various track forms are also presented to give insight into the differences in acoustic performance. The models allow the relative contributions of the track and wheels to the pass-by noise to be identified. In addition the effect of rail dampers added to the slab track is assessed. These attenuate the noise at higher frequencies due to the increase in decay rate, but an increase in radiation is noted at 500 Hz and below, possibly linked to differences in effective roughness.

Keywords: Tram tracks; Rolling noise; Track decay rate; Rail roughness; Sound radiation; Rail damper.

1 Introduction

Tramways are becoming a popular means of urban transport which can help to overcome the increasing traffic congestion and pollution found in many cities. Although their speed of operation is relatively low compared with conventional railways, tramways can nevertheless produce significant levels of noise and consequent annoyance [1-2]. This is partly a result of

their close proximity to sensitive receivers but is also a consequence of the high levels of rail roughness and corrugation often found on tram networks [3-4]. Local defects such as rail joints, switches or wheel flats can also have influence by causing impact noise [5]. As well as airborne noise, ground-borne vibration and noise can also be sources of annoyance [6].

The generation and propagation of rolling noise from tramways can be affected by various factors such as wheel design, track type and the acoustic properties of the ground. Different types of track are used for tramways, including conventional ballasted tracks, concrete slab tracks and paved-in tracks for street running. Examples are shown in Figure 1. Although the rolling noise of conventional railways has been studied extensively [7], including research into the generation mechanisms, the development of models such as TWINS [8] and the implementation of various noise control methods [9], much less attention has been given to tramways.

(a) (b) (c)

Figure 1. Tramway track forms: (a) ballasted track, (b) slab track with embedded sleeper blocks, (c) embedded track in grass.

Pallas et al. [10] studied the noise sources on two different types of tram in France, using microphones in an arc to determine the sound power and directivity as well as a two-dimensional microphone array to localise sources on the tram. Measurements were made on two different types of embedded track, one located in the street and the other surrounded by grass. The results showed that the rolling noise was the most important source and that this was more affected by the track type than the vehicle type; the street-running track had softer rail pads and had noise levels 6-10 dB(A) higher than the track in grass which had stiffer pads.

Mandula et al. [11], and more recently Panulinova [12], developed empirical models for tramway noise based on measurements in Slovakia in which some differences were noted between different track forms. Olafsen and Stensland [13] presented results of noise monitoring in Oslo from which an empirical model for tram noise has been developed. Account was taken of the time since rail grinding and the overall corrugation amplitude. Different track types were distinguished: ballasted track, street running and ‘green track’. Street tracks were on average 1

dB(A) noisier than ballasted tracks and 2.5 dB(A) noisier than green tracks. Spectral differences were also presented.

Rezac and Skotnicova [14] investigated the effects of introducing an absorptive treatment on the surface of a concrete tram track by using recycled rubber. The effect on the overall A-weighted sound was negligible but a reduction of 2-3 dB was found in the sound level for frequencies above 500 Hz.

Lakusic et al. [15] presented measurements of noise levels from trams in Croatia for different track fastening systems. A system with double elastic layer was shown to produce noise levels up to 3 dB(A) lower than one with a single rail pad. However, no spectral information was presented. In [16] Lakusic et al. compared two new constructions of street-running track with an existing track form. Decay rates were obtained from pass-by measurements. The lowest noise levels corresponded to the track with the highest decay rates. The two new track forms were 1.6 and 3.6 dB(A) quieter than the existing track design. No account was taken of rail roughness although the track sections were all newly constructed so differences in roughness can be expected to be small.

Byrne [17,18] studied the effects of rail grinding on the noise from trams on the Luas network in Dublin. Significant corrugation was found prior to grinding. Noise reductions due to grinding ranged from 4 dB(A) on an embedded track to 12 dB(A) at a location on a slab track. In [19], Byrne described tests with rail dampers and absorptive rubber mats applied on slab track sections. Preliminary results indicated that the absorptive mats reduced the pass-by noise by 2.5-4 dB(A) and the rail dampers by 2-3.5 dB(A).

Jolibois et al. [20] described an experimental low barrier placed next to a tram line. The barrier was 0.95 m high and formed of an inverted L with absorptive material mounted on the inside faces. Noise levels were measured directly behind the barrier at a distance of about 4.5 m from the centre of the nearest track and at heights of 1.2 and 1.5 m. Reductions were on average more than 10 dB(A) for trams on the closest track and 7.5 dB(A) for the far track.

Embedded tracks, commonly used on tramways, require a different modelling approach from conventional open rails. Nilsson et al. [21] introduced a waveguide finite element (FE) and boundary element (BE) modelling approach and applied it to a comparison of an open rail and an embedded tram rail. Such a modelling approach, also known as a 2.5D method, is applicable to structures where the geometry and material properties are constant along one coordinate direction. It involves a two-dimensional FE/BE model which is solved for a series of wavenumbers in the third dimension.

Zhao et al. [22] presented finite element and boundary element models of a finite length of embedded rail track. These models were validated using measured results and the track design was optimised for reduced noise using the calculation models by changing the shape of the embedding cross-section and its material properties.

Trams often use resilient wheels which are generally quieter than mono-block steel wheels. Bouvet et al. [23] presented a numerical study of resilient wheels. Although this was not focused on tram applications it gave some insight into how resilient wheels can be optimised to reduce the rolling noise from both the wheel and the track.

The aim of this paper is to compare the rolling noise of trams running on different tracks and to identify the reasons for the differences between them. A systematic comparison is carried out of four different tracks on a single network, through both measurements and prediction models. These are a ballasted track, a slab track with embedded sleeper blocks, a track with embedded rails in grass and a slab track fitted with rail dampers. To take account of the field conditions, measurements of rail and wheel roughness and track decay rates have been carried out; these are described in Section 2. Calculation models for the different tracks are presented in Section 3. For ballasted and slab tracks these are based on the TWINS model [8] while for the embedded rail a wavenumber domain method [21,24] is used. Comparisons are made with measured mobilities and decay rates. In Section 4 measured and predicted noise spectra are presented, and the various tracks are compared allowing for differences in roughness. In Section 5 the effect of applying rail dampers to the slab track is discussed.

2 Roughness and track decay rates of different tram tracks

Measurements have been carried out on several different tram tracks located on a single European tram network. These include a conventional ballasted track, a slab track with embedded sleeper blocks and an embedded rail in grass, as shown in Figure 1. In addition a slab track fitted with rail dampers was also measured. In this Section, measurements of rail and wheel roughness and track decay rate are described.

2.1 Rail and wheel roughness

The roughness on both rails of each site over a length of 150 m was measured using the CAT system and processed into one-third octave band spectra [25]. The average spectrum for each site is presented in Figure 2. The reference curve from ISO 3095:2013 [26] is also shown for comparison. The rail roughness spectra at all locations are quite similar and they are all

considerably higher than the ISO reference curve, with differences of more than 20 dB. There is no distinct peak in these roughness spectra although some visible short wavelength corrugation was observed. The roughness of the slab track is slightly lower than the others, possibly because it had been ground more recently. Figure 2 also shows the roughness measurement results for the slab track section fitted with rail dampers which will be discussed in Section 5. It can be seen that there is very little difference between the slab track sites with and without the rail dampers.

In addition, the roughness of 8 wheels from a single tram was measured in the rolling stock depot. These measurements included both powered and unpowered bogies although no significant differences were observed between them. The average wheel roughness spectrum is included in Figure 2. The wheel roughness is lower than the rail roughness, with a difference of more than 10 dB for wavelengths greater than 20 mm. It is assumed that this spectrum is representative of the trams from which noise and vibration have been measured.

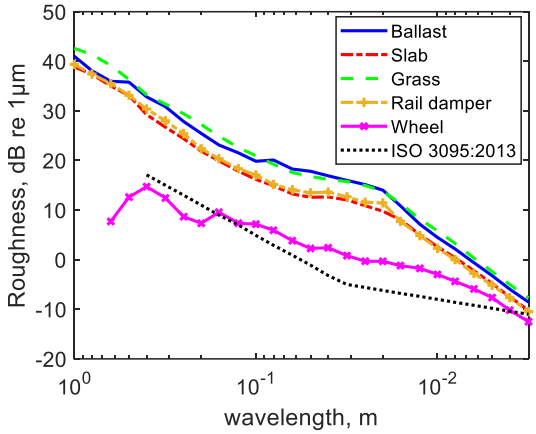

Figure 2. Rail roughness measured on different types of tram track and wheel roughness.

2.2 Track decay rate

The track decay rate has been measured using the method in EN 15461 [27] using impact hammer excitation. The results are presented in Figure 3(a) for the vertical direction and Figure 3(b) for the lateral direction. In the case of the embedded rail the lateral direction could not be measured as the rail was not accessible. The corresponding reference curves from ISO 3095:2013 [26] are shown for comparison.

The ballasted track site has the highest vertical decay rate over much of the frequency range. This and the slab track were fitted with relatively stiff rail pads. In contrast, the embedded rail has a relatively low support stiffness leading to a lower decay rate than the ballasted track between 400 and 1250 Hz. The slab track has resiliently mounted sleeper blocks

and its vertical decay rate is very similar to that of the ballasted track above 1250 Hz but it is lower between 250 and 1000 Hz. The lateral decay rates of the ballasted track and slab track are very similar for all frequencies above 200 Hz. The addition of the rail dampers to the slab track increases the track decay rate in the vertical direction between 500 and 1000 Hz and in the lateral direction for much of the frequency range.

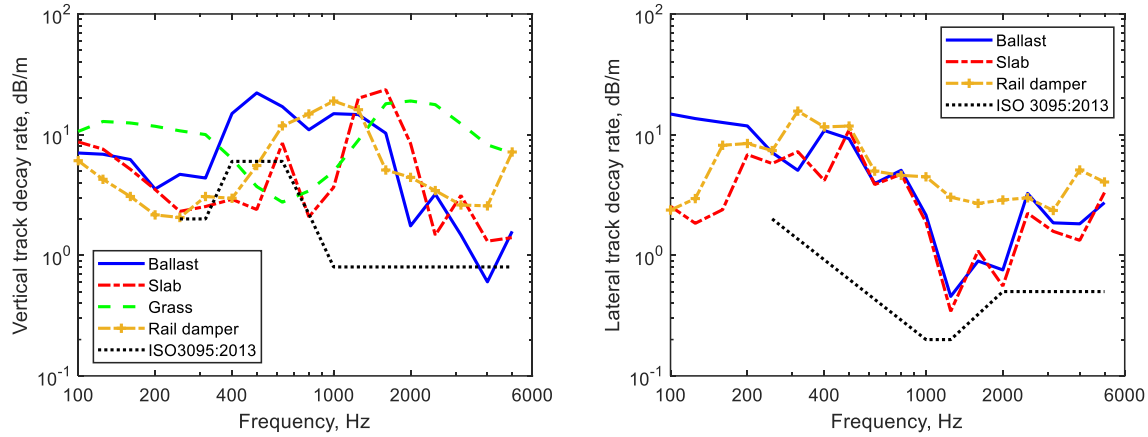

(a) (b)

Figure 3. Measured track decay rates on ballast, slab, grass track and slab track with rail damper. (a) Vertical; (b) lateral.

3 Vibro-acoustic models of different tram tracks

3.1 Track models of ballast and slab track

The ballasted track and slab track shown in Figure 1(a,b) are both fitted with S49 rails (49 kg/m); their cross-sections are shown in Figure 4. They are both modelled here using a discretely supported Timoshenko beam for the rail [7]. The ballasted track has monoblock sleepers, which are modelled using beam elements, whereas the slab track has embedded sleeper blocks, which are represented as lumped masses. The main parameters used for these two tracks are listed in Table 1. The rail pad parameters have been identified by fitting the model to the measured track mobilities and decay rates.

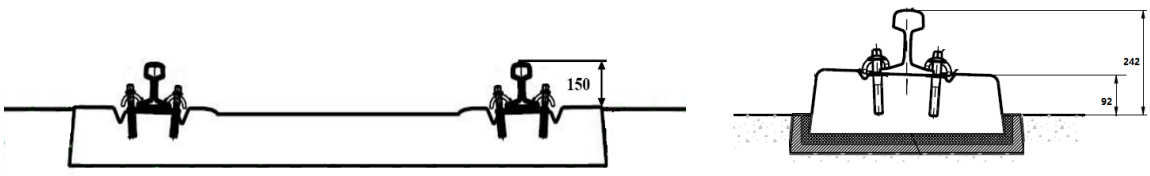

(a) (b)

Figure 4. Open forms of tram track; (a) ballasted track; (b) slab track with embedded blocks.

Table 1. Parameters of ballast and slab tracks

	Parameter	Ballast	Slab
Rail	Rail type	S49 Rail	
	Vertical bending stiffness	3.81MN.m^2	
	Lateral bending stiffness	0.67 MN.m^2	
	Mass per unit length	49 kg/m	
	Shear coefficient	0.4	
	Damping loss factor	0.02	
Subgrade	Subgrade type	Ballast	Slab
Sleeper	Sleeper type	Mono-block	Booted sleeper
	Sleeper model	Beam	Mass
	Sleeper mass	192 kg	40 kg (per side)
	Sleeper spacing	0.755 m	0.755 m
Rail pad	Vertical stiffness	1500 MN/m	1500 MN/m
	Lateral stiffness	300 MN/m	150 MN/m
	Vertical loss factor	0.2	0.4
	Lateral loss factor	0.2	0.2
Ballast / Booted rubber pad (slab track)	Vertical stiffness	Frequency dependent [28]	80 MN/m
	Lateral stiffness	100 MN/m	15 MN/m
	Vertical loss factor	1.0	0.4
	Lateral loss factor	1.0	0.15

The measured and predicted point mobilities of the ballasted track at mid-span between sleepers are compared in Figure 5 for vertical and lateral directions. The predictions show a good agreement with the measured data. The peak at around 800 Hz in the vertical mobility is the ‘pinned-pinned’ resonance frequency and also coincides with the resonance of the rail mass bouncing on the rail pad stiffness. The predicted lateral mobility is lower than the measurement as the model does not include torsion or cross-section deformation.

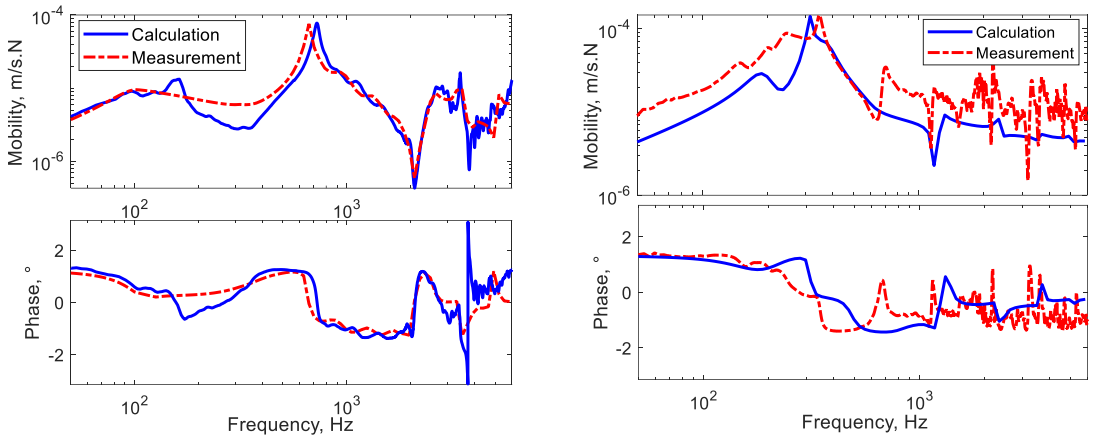

Figure 5. Rail point mobilities at mid-span of ballasted track from calculation and measurement. (a) Vertical; (b) lateral.

The track decay rates calculated with the track model are compared with the measurement results in Figure 6. These show the correct trends although there are differences of detail.

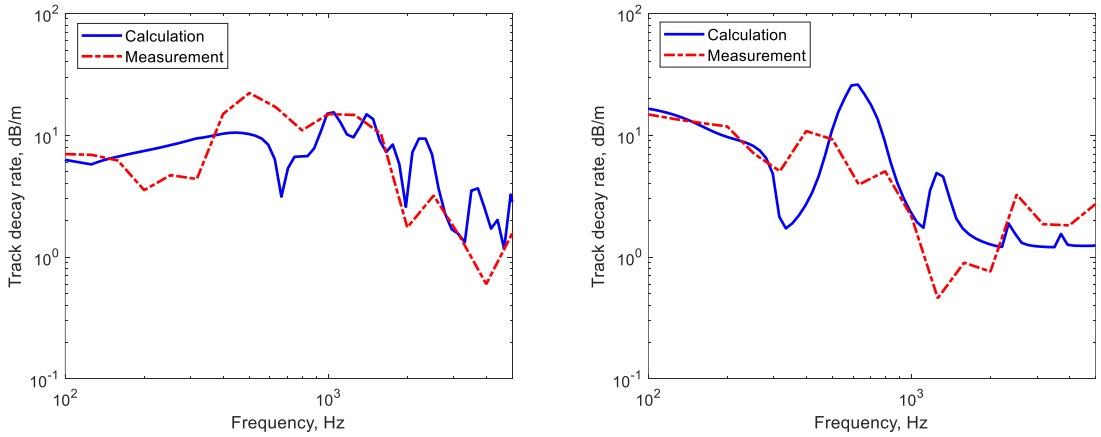

Figure 6. Track decay rates of ballasted track from calculation and measurement. (a) Vertical; (b) lateral.

Figure 7 compares the calculated and measured mobilities of the slab track. Good agreement is again found, especially for the vertical direction. Figure 8 shows the corresponding track decay rate results which give reasonable agreement for both directions.

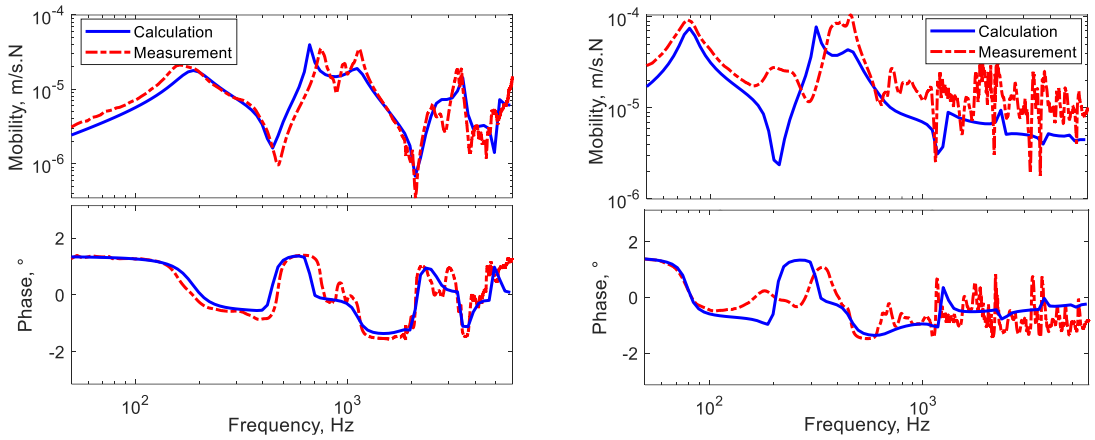

Figure 7. Rail point mobilities at mid-span of slab track from calculation and measurement. (a) Vertical; (b) lateral.

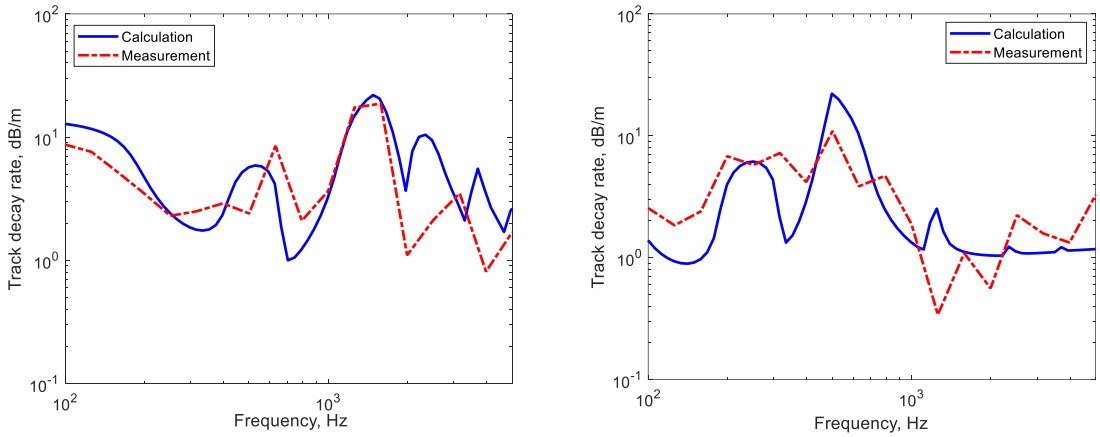

Figure 8. Track decay rates of slab track from calculation and measurement. (a) Vertical; (b) lateral.

3.2 Embedded track model

The embedded track studied here (Figure 1(c)) is shown schematically in Figure 9. It consists of 59R2 groove rail which is pre-coated with a rubber embedding material and then cast into the concrete slab. The filling material has an influence on both the rail vibration and its sound radiation [21,24]. Between the rails and outside them the track surface is covered in grass. The absorptive effect of the grass should therefore also be taken into account.

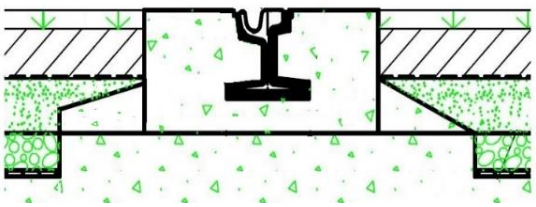

Figure 9. Embedded track form of tramway: embedded track with grass.

A 2.5D FE/BE model of the embedded track has been created similar to that presented by Nilsson et al. [20]. More details are given in [24]. Different models are used for low and high frequencies to ensure that the elements are small compared with the structural wavelength. The groove rail and embedding material are discretised in each case using solid elements. For frequencies below 1000 Hz the surrounding concrete is also included in the FE model and elastodynamic boundary elements along the bottom of the slab are used to represent the support from the underlying ground. At higher frequencies the model does not include the concrete as its contribution is found to be negligible due to the vibration isolation effect of the embedding material. The material properties used in the model are listed in Table 2. The normal velocity of the upper surface of the model is used as input to a 2.5D acoustic BE model to calculate the sound radiation. At low frequencies this includes the vibration of the concrete as well as the rail and embedding material.

Table 2. Parameters of embedded track [24]

Parameter	Rail	Embedding material	Concrete	Soil
Young's modulus (MPa)	211000	4.2	43000	107
Density (kg/m^3)	7850	1500	2500	1835
Poisson's ratio	0.3	0.45	0.15	0.30
Damping loss factor	0.02	0.25	0.01	0.04

A unit vertical force is applied on the middle of the rail surface and the point mobility of the rail is shown in Figure 10(a), together with the measurement result. It shows a good agreement over the whole frequency range. The peak at around 350 Hz is the resonance frequency of the rail bouncing on the stiffness of the filling material support.

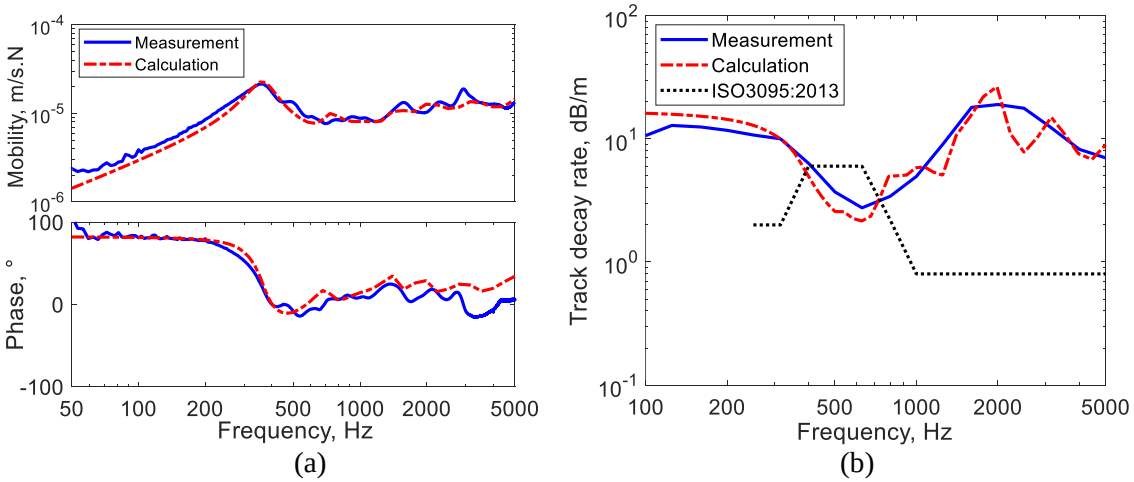

Figure 10. Comparison between measurement and calculation of embedded tracks. (a) Mobility; (b) track decay rate.

The vertical track decay rates are calculated using transfer mobilities from the model, following the same procedure as in the measurement [27]. These are compared with the measurement results in Figure 10(b). At low frequencies, the track decay rate is very high due to the stiffness of the filling material. It drops above about 350 Hz, which corresponds to the resonance seen in Figure 10(a). At high frequencies, the track decay rate increases again due to the damping effect of the filling material. Good agreement is found with the measurement over the whole frequency range.

3.3 Dynamic responses of wheel

The dynamic responses of the tram wheel were also measured. These were resilient wheels with a radius of 0.3 m. The wheel was lifted clear of the rail and was excited using a small impact hammer. The response was measured using an accelerometer attached using wax. By exciting at different positions, these measurements were used to identify the main wheel modes. The mobilities were also predicted using a finite element model and the properties of the resilient layer were adjusted to give good agreement in terms of natural frequencies. Modal damping ratios were also chosen according to the measurement; for the modes with two or more nodal diameters, occurring above 600 Hz, these were between 0.2% and 0.5%.

Figure 11 shows the measured and predicted radial and axial mobilities of the resilient wheel at the nominal contact point. Both the radial and axial wheel mobilities from the FE model show a good agreement with the measured results over the whole frequency range, confirming the validity of the FE model. There is a small difference in the radial mobility at the first peak at around 100 Hz. The prominent modes at 667 Hz and 900 Hz are axial and radial modes with two nodal diameters, 1746 Hz and 2313 Hz are axial and radial modes with three nodal diameters, 3132 Hz and 3230 Hz are axial and radial modes with four nodal diameters.

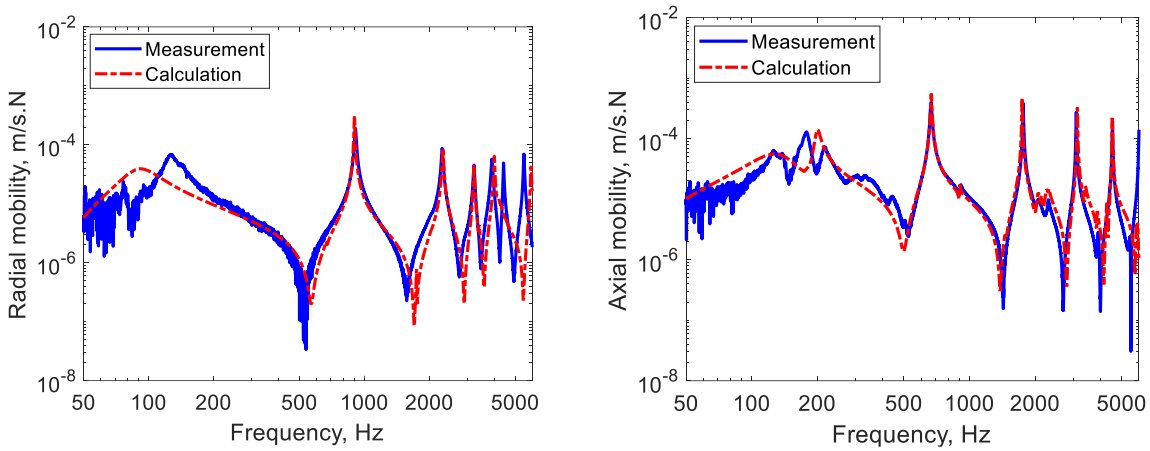

Figure 11. Mobility magnitude of resilient wheel. (a) Radial; (b) axial.

3.4 Sound radiation of rails

The ground around the track has an influence on the sound power radiated by the track through its acoustic impedance [29] in addition to its effect on the sound propagation from both track and wheel noise sources [30]. The sound power emitted by the rail is calculated taking account of the different source properties of the rail above sleepers and between sleepers according to the model proposed in [30, 31]. As seen in Figures 1, 4 and 9 the three tracks have different ground materials and heights of the rail relative to the ground. For the slab track, due to the 'booted' sleepers, the total height from the rail head to the ground is 242 mm. For the ballasted track, the sleepers are embedded in the ballast and the corresponding height is approximately 180 mm. The groove rail is embedded in the ground and the rail head is at the same level as the ground. The influence of the ground on the sound power radiated by the rail can be considered by using an acoustic impedance model in the BE model of the rail radiation [31]. For simplicity the Delany-Bazley model [32] is used to obtain the frequency-dependent impedance according to the equivalent flow resistivity of the ground. To determine the sound power radiated by the rail, the slab surface is assumed to be rigid at a height of 92 mm below the rail foot, whereas the ballast is represented by a flow resistivity of 30 kPa.s/m^2 [30] and the grass ground is represented by a flow resistivity of 300 kPa.s/m^2.

The calculated sound power per unit length, normalized by the squared velocity of the rail head averaged over the length, is shown in Figure 12 for the different tracks. The embedded rail acts like a line monopole source, which leads to a higher sound power at low frequencies than the open rail. Additionally, the embedded rail has a greater radiating area at low frequencies due to the contribution of the concrete surrounding the rail. For the ballasted track

the rail has a slightly lower normalized sound power than for the slab track above 300 Hz due to the effect of the absorptive properties of the ballast on the source [30].

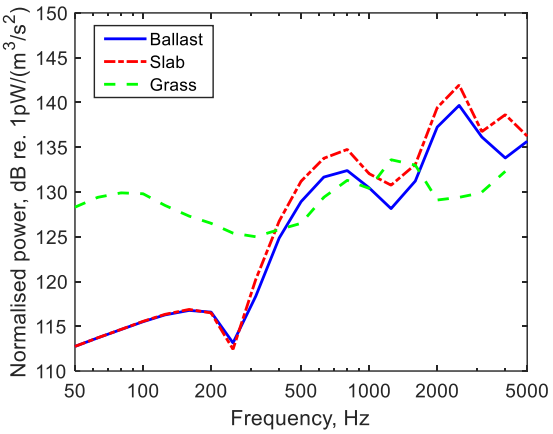

Figure 12. Sound power normalised by the squared velocity of rail of different tracks.

3.5 Insertion loss of bogie region

The bogie region of the trams is enclosed by side skirts which come down to within 205 mm of the rail head, see Figure 13(a). To give an indication of the shielding effect of these skirts a simple diffuse field model of an enclosure is used here [33]. The track and wheels are assumed to radiate into this cavity and the power balance equation is used to equate the input power to the sum of the dissipated power and the power emitted through the gaps. Consequently, the insertion loss of the cavity can be written as [34]

$$\mathrm{IL} = 10\log_{10}\left(\frac{S_{\mathrm{abs}}+S_{\mathrm{ap}}}{S_{\mathrm{ap}}}\right) \tag{1}$$

where S_{ap} is the surface area of the apertures and S_{abs} is the absorption area within the cavity, i.e. the absorption coefficient multiplied by the surface area. The absorptive areas within the cavity include the ground and the underside of the tram. For the ground, the measured absorption coefficient of ballast [30] is used for the ballasted track; for the grass ground the absorption coefficient is derived from the Delany-Bazley model [32] with an equivalent flow resistivity of 300 kPa.s/m^2; the surface of the slab track is taken as rigid. The absorption coefficient of the underside of the tram is taken as 0.25.

The insertion loss of the bogie cavity estimated using this simple approach is shown in Figure 13(b) for these three surfaces, and can be seen to vary between 2 and 6 dB. The gap height below the bottom of the vehicle skirt, shown as H in Figure 13(a), is taken as 205 mm for the grass ground, 385 mm for the ballasted track and 447 mm for the slab track. This,

together with the differences in absorption, leads to the grass ground having the highest insertion loss and the slab track the lowest one. The difference between the grass track and the slab track is between 2 and 4 dB. The wheel/rail noise is assumed to be reduced by this insertion loss to determine the sound pressure level at the receiver.

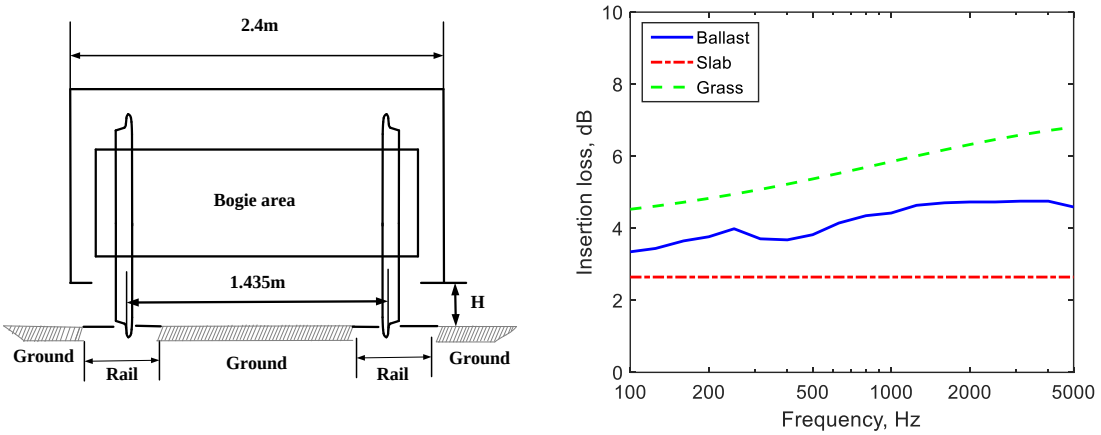

(a) (b)

Figure 13. The influence of tramcar bogie cavity. (a) Schematic cross-section view of bogie cavity; (b) insertion loss of bogie cavity for different tracks.

4 Rolling noise predictions and measurements

Simultaneous measurements were taken of rail vibration and noise at the trackside during tram passages at each site. The total length of each tram was 54 m with 10 wheelsets. The measured speeds for the different tracks were all close to 55 km/h. The noise measurement location in each case was 7.5 m from the track centreline and 1.2 m above the rail head [26]. The geometrical parameters used in the model are listed in Table 3. The track sections were all in relatively free field conditions although the slab track was on a concrete viaduct. The effect of the rail dampers is considered separately in Section 5 below.

Table 3. Parameters used for source heights and ground (all heights relative to the top of the rail)

	Ballasted	**Slab**	**Grass**
Wheel source height (m)	0.1	0.1	0.1
Rail source height (m)	–0.075	–0.075	0
Sleeper source height (m)	–0.149	–0.149	–
Ground height (m)	–0.2	–0.242	0

Figure 14 shows noise spectra for the ballasted track. These and subsequent figures show unweighted spectra, although overall A-weighted levels are also listed. The conventional reference value of 20 μPa is used for sound pressure level throughout. In Figure 14(a), the

predictions from the TWINS model (including the effect of the insertion loss from the previous section) are compared with the measured spectra. The measured track decay rates are used in the TWINS predictions. A range of measured spectra is given based on five tram passages with speeds of 55±5 km/h. Generally good agreement is found. The background noise spectrum is also shown, which can be seen to be much lower than the measured spectra. In Figure 14(b) the contributions of the wheels, rails and sleepers to the predicted noise spectra are shown. The rail and wheel components of noise are similar to each other at low frequencies and around 1000 Hz. The peak in the wheel noise in the 1 kHz band corresponds to a radial mode seen in Figure 11(a). For a stiff rail pad such as used here, the sleeper is strongly coupled to the rail for frequencies up to at least 1000 Hz. However, the inclusion of the discrete supports means that the pinned-pinned frequency also occurs at around this frequency. Consequently, the rail vibration is much larger at mid-span than it is above the sleepers for frequencies between 400 and 1500 Hz, so the average rail vibration is greater than the sleeper vibration in this frequency region and the noise from the sleepers is the dominant source only for frequencies below 300 Hz.

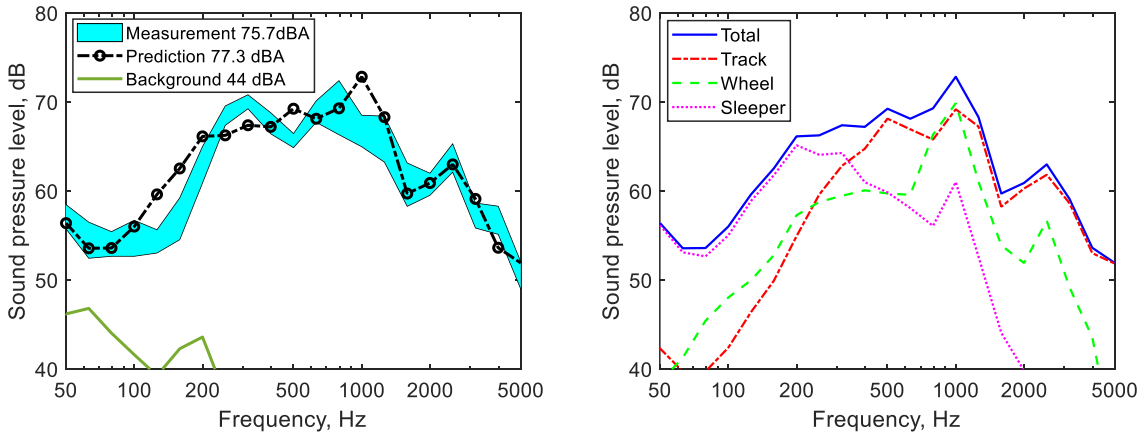

(a) (b)

Figure 14. Rolling noise of ballasted tramway track; (a) Comparison of TWINS prediction and measured noise; (b) contributions to the predicted noise from different components noise.

Figure 15 shows corresponding results for the slab track. Here, the background noise is relatively high at low frequencies but is not significant above 250 Hz. In this low frequency region, noise from the viaduct may also contribute but this is not relevant to the A-weighted levels. The measurements correspond to three tram passages with speeds of 56±4 km/h and contain quite a lot of variability, especially at low frequency due to the high background noise.

The predicted spectrum is slightly higher than the measured one between 500 and 1250 Hz. For this track the noise level from the rail and the sleeper blocks is higher than for the ballasted track.

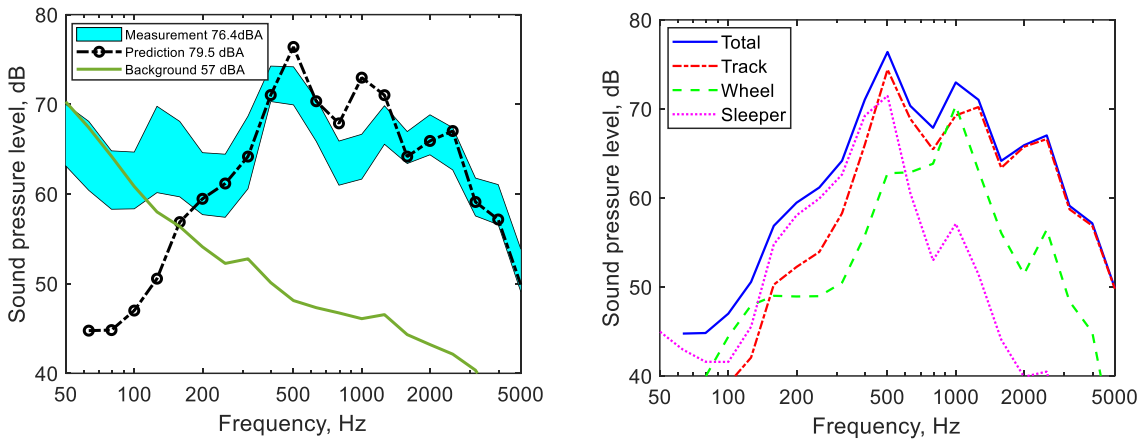

(a) (b)

Figure 15. Rolling noise of slab tramway track; (a) Comparison of TWINS prediction and measured noise; (b) contributions to the predicted noise from different components.

Figure 16 shows results for the embedded track. In this case measurements of four trams are included, with speeds of 56±3 km/h. Good agreement is obtained between the predictions and the measurements over most of the frequency range although the predictions are too low at 2 kHz and above, which may be due to inadequacies in the simple model of the bogie cavity. Especially for the wheel noise there may be some direct radiation to the exterior, whereas in the model it is assumed that all sound is radiated into the bogie cavity.

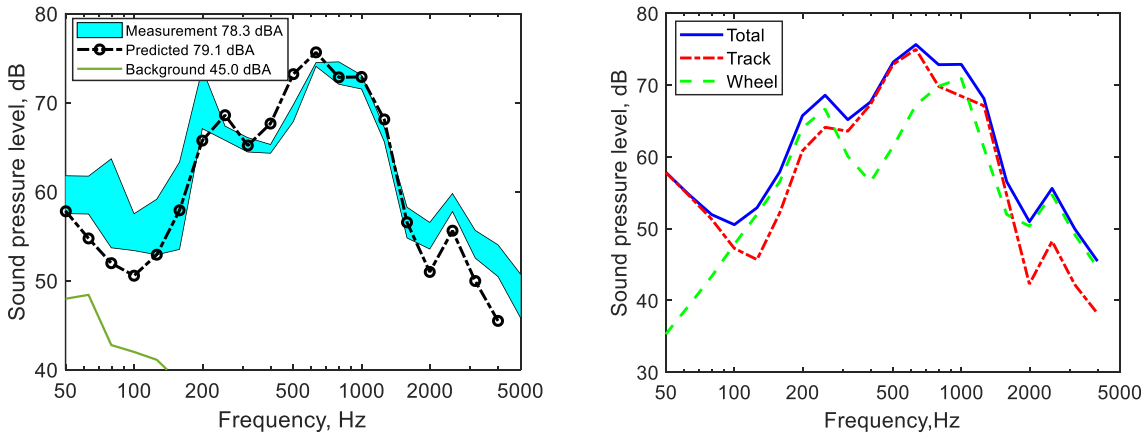

(a) (b)

Figure 16. Rolling noise of grass tramway track; (a) Comparison of prediction and measured noise; (b) contributions to the predicted noise from wheel and track.

Some differences were observed between the roughness spectra for each location in Figure 2. To allow for these differences, measured and predicted noise spectra have been corrected to correspond to the same roughness spectrum and tram speed. These are shown in Figure 17. When presented in this form it is clear that the slab track is the noisiest in both the measurements and the predictions, with levels that are higher than the ballasted track over much of the frequency range. The noise level from the grass track is more similar to that of the ballasted track although the spectra are different.

The overall A-weighted noise levels from these results are listed in Table 4 along with the predicted contributions from each component. The overall level for the slab track is 3-5 dB higher than for the ballasted track, mainly due to a higher noise level from the rail. The cavity insertion losses (Figure 13(b)) also affect these differences. The rail noise component is 3 dB greater than the wheel noise for the ballasted track and 5 dB greater for the slab track. For the grass track, the overall level is 1-2 dB higher than for the ballasted track in both the measurements and the predictions.

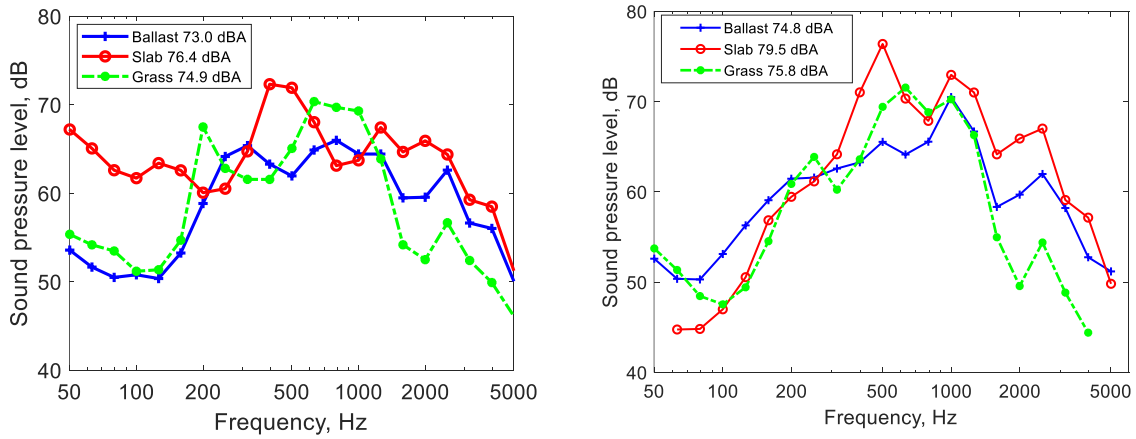

(a) (b)

Figure 17. Noise spectra for different tram tracks after normalizing to the same roughness and the same speed. (a) Measurement results; (b) calculation results.

Table 4. A-weighted sound pressure levels at 7.5 m from track centreline for different tracks normalized to the roughness of the slab track at a speed of 56.2 km/h

Track type	Total - average measurement (dBA)	Total - predicted (dBA)	Rail (dBA)	Wheel (dBA)	Sleeper (dBA)
Ballast	73.0	74.8	72.6	69.9	63.1
Slab	76.4	79.5	77.7	72.8	70.7
Grass	74.9	75.8	73.8	71.4	/

5 The influence of rail dampers on the noise from the slab track

As noted in Section 4, the slab track has the highest levels of noise. Rail dampers had previously been fitted to one section of the slab track and preliminary results were discussed in [19]. In this Section, additional measurements are used to assess the effect of the rail dampers on the noise from the slab track. The site is shown in Figure 18.

Figure 18. Slab track site fitted with rail dampers.

The measured point mobilities of the slab track with and without rail dampers are compared in Figure 19. With the rail dampers, the peaks in the vertical mobility are less pronounced than without them, especially in the frequency range between 630 Hz and 1250 Hz. The low frequency peak in the vertical mobility is shifted from about 175 Hz to 120 Hz due to the added mass of the dampers. Similar changes are seen in the lateral mobility.

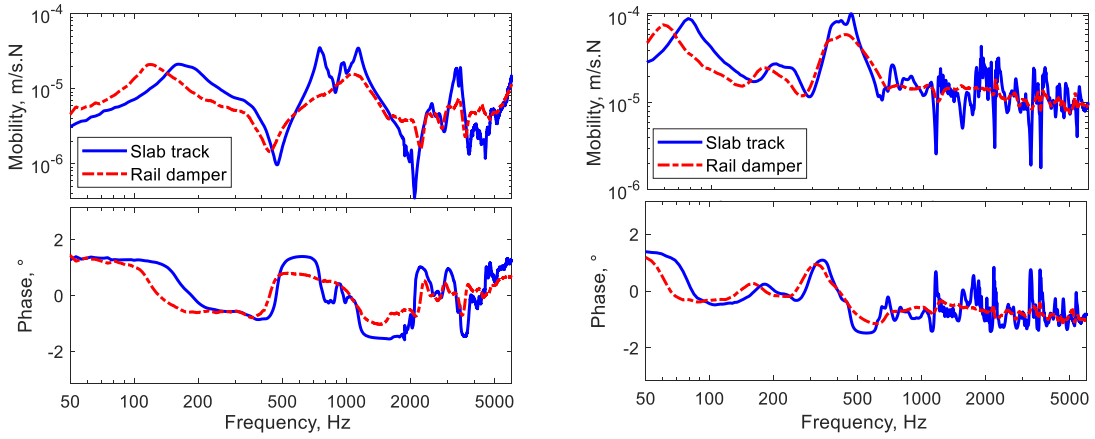

Figure 19. Mobility magnitude and phase of slab track measured at mid span with and without rail dampers. (a) Vertical; (b) lateral.

The rail vibration was measured during tram passages and is shown in Figure 20 in the form of velocity spectra. For the lateral direction, it can be seen from Figure 20(b) that the rail dampers reduce the rail vibration over a wide frequency range. The vertical rail vibration above 630 Hz is also much lower with the rail dampers than without them. However, between 200 Hz

and 500 Hz the vertical rail vibration is greater in the case with rail dampers. The reason for this is unclear; the measured roughness is similar (Figure 2) and the track decay rate is slightly higher with the dampers (Figure 3(a)). One possibility is that variations in the rail roughness across the railhead are not reflected in the roughness measurements. These were taken along a single line, which was located as best as possible in the centre of the running band.

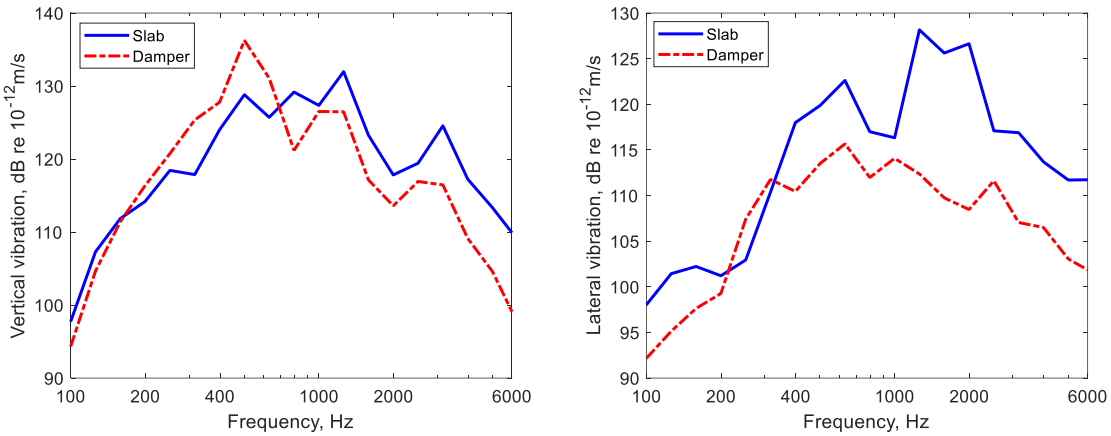

Figure 20. Measured rail vibration velocity of slab tracks with and without rail dampers for tram pass-bys at speed of around 55 km/h. (a) Vertical; (b) lateral.

Figure 21 shows the measured noise spectra with rail dampers, averaged over two train passages, compared with the average for the slab track without dampers from Figure 17(a). These have been normalised to the same roughness, although as noted in Figure 2 the differences in roughness were small. They show a similar trend to the vertical rail vibration in Figure 20(a). The average noise of the track with rail dampers is only 0.2 dB(A) lower than that without. However, this is strongly influenced by the peak at 500 Hz. From the noise spectrum result, it can be seen the rail damper can reduce the noise very effectively for frequencies above 630 Hz; the overall A-weighted noise level for 800-5000 Hz is reduced by 3.4 dBA.

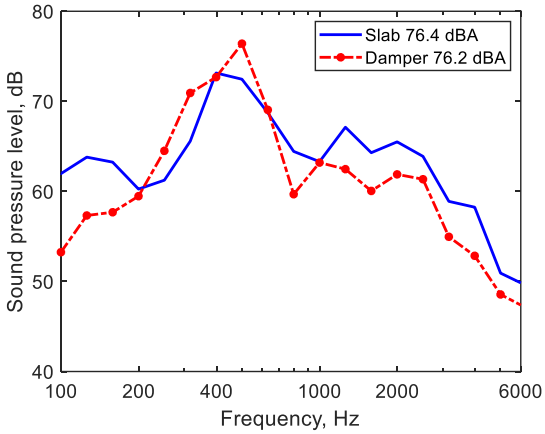

Figure 21. Noise measurement result normalized to the same slab track roughness at speed 56.2 km/h.

6 Conclusions

The influence of track design on the rolling noise from tramways has been studied through a systematic comparison of different tracks on a single tram network. These include a ballasted track, a slab track with booted sleeper blocks, and a track with embedded rails and grass surface. Measurements of rail and wheel roughness have been carried out, as well as track decay rates, rail and wheel mobility, rail vibration and pass-by noise. In common with other tram systems, high levels of rail roughness are found on all the tracks.

The ballasted track site has the highest vertical decay rate over much of the frequency range, whereas the vertical decay rate of the grass track is quite low between 400 and 1250 Hz but larger at high frequencies. After normalizing the noise spectra to the same roughness and speed the ballasted track is found to be the quietest of the tracks studied here. This is mainly because of its high track decay rate and the absorptive effect of the ballast. The noise levels from the slab track are 3-4 dB higher than the ballasted track, the main contribution being from the rail. The noise from the grass track is also quite high, about 2 dB higher than for the ballasted track, due to its low track decay rate in the important middle frequency range.

Theoretical models of the various track forms have also been used to give insight into the differences in acoustic performance. Reasonable agreement is found with the measured mobilities and decay rates, particularly for the vertical direction. A simple model of the bogie cavity has also been used to give an indication of the insertion loss of the vehicle skirts and the absorptive effect of the ground. The models also allow the relative contributions of the track and wheels to the pass-by noise to be identified. For the slab track the component of noise from the track is estimated to be around 5 dB greater than that of the wheel, whereas for the ballasted and grass tracks the difference is around 3 dB. The results are influenced by the insertion loss

of the bogie cavity which has been estimated using a simple model to vary between 2 and 6 dB, with differences between the tracks of 2-4 dB. Better estimates of this and the effect of ground absorption are required in future.

Rail dampers attached to the slab track are found to reduce the noise above 800 Hz by 3.4 dB(A). However, a peak is found in the rail vibration at 500 Hz which means that the track with dampers in this case is no quieter in terms of overall A-weighted level, possibly due to higher effective rail roughness that has not been accounted for.

Acknowledgements

The work described here has been supported by the EPSRC United Kingdom under the programme grant EP/M025276/1, 'The science and analytical tools to design long life, low noise railway track systems (Track to the Future)'. This work was carried out while the first author was working at ISVR, University of Southampton, sponsored by the CSC Program of China. All data published in this paper are openly available from the University of Southampton repository at: 10.5258/SOTON/D1472.

References

[1] S. Sandrock, B. Griefahn, T. Kaczmarek, H. Hafke, A. Preis, T. Gjestland. Experimental studies on annoyance caused by noises from trams and buses. J. Sound Vib 2008; 313(3-5): 908-919.

[2] A. Trollé, C. Marquis-Favre, A. Klein. Short-term annoyance due to tramway noise: Determination of an acoustical indicator of annoyance via multilevel regression analysis. Acta Acust. United Acust 2014; 100(1): 34-45.

[3] L. Chiacchiari, D.J. Thompson, G. Squicciarini, E. Ntotsios and G. Loprencipe. Rail roughness and rolling noise in tramways. Journal of Physics: Conference Series, Vol. 744. No. 1. IOP Publishing; 2016.

[4] S.L. Grassie. Rail irregularities, corrugation and acoustic roughness: characteristics, significance and effects of reprofiling. J Rail Rapid Transit; 2012; 226: 542-557.

[5] G. Kouroussis, S.Y. Zhu, B. Olivier, et al. Urban railway ground vibrations induced by localized defects: using dynamic vibration absorbers as a mitigation solution. J. Zhejiang Univ.-SCI A; 2019, 20: 83-97.

[6] D.J. Thompson, G. Kouroussis, E. Ntotsios. Modelling, simulation and evaluation of ground vibration caused by rail vehicles. Veh. Syst. Dyn.; 2019, 57: 936-983.

[7] D. Thompson. Railway Noise and Vibration: Mechanisms, Modelling and Means of Control. Elsevier: Oxford, UK ;2009.

[8] D.J. Thompson, B. Hemsworth, N. Vincent. Experimental validation of the TWINS prediction program for rolling noise, part 1: description of the model and method. J. Sound Vib 1996; 193: 123-135.

[9] D.J. Thompson and P.E. Gautier. A review of research into wheel/rail rolling noise reduction, Proc. Instn Mech. Engrs Part F, J Rail Rapid Transit, 2006;220F; 385-408.

[10] M.A. Pallas, J. Lelong, R. Chatagnon. Characterisation of tram noise emission and contribution of the noise sources. Appl. Acoust 2011; 72: 437-450.

[11] J. Mandula, B. Salaiová, M. Koval'akova. Prediction of noise from trams. Appl. Acoust 2002; 63:373-389.

[12] E. Panulinová. Input data for tram noise analysis. Procedia Engineering (Structural and Physical Aspects of Construction Engineering) 190 (2017) 371-376.

[13] S. Olafsen, A. Stensland, Tram noise monitoring. Baltic-Nordic Acoustics Meeting, 15-18 April 2018, Harpa, Reykjavik, Iceland.

[14] M. Rezac, I. Skotnicova. Noise attenuation from tramway traffic. Communications - Scientific Letters of the University of Zilina 2012; 14(4): 73-78.

[15] S. Lakusic, V. Dragcevic, T. Rukavina, The impact of tram track fastening systems on noise level. WIT Transactions on The Built Environment 2005; 77: 487-497.

[16] S. Lakusic, I. Haladin, M. Ahac, The effect of rail fastening system modifications on tram traffic noise and vibration. Shock Vib 2016; paper 4671302.

[17] S. Byrne, An investigation into noise emissions following a rail grinding campaign on Dublin's light rail system. International Congress on Sound and Vibration, London 23-27 July 2017.

[18] S. Byrne, Reductions in environmental noise emissions from Dublin's light rail system following a rail grinding campaign on embedded track. Euronoise 2018, Crete, 27-31 May 2018.

[19] S. Byrne, An assessment of the effectiveness of noise reduction systems on Dublin's light rail system (Luas). Euronoise 2018, Crete, 27-31 May 2018.

[20] A. Jolibois, J. Defrance, H. Koreneff, P. Jean, D. Duhamel, V.W. Sparrow, In situ measurement of the acoustic performance of a full scale tramway low height noise barrier

prototype. Appl. Acoust 2015; 94: 57-68.

[21] C.M. Nilsson, C.J.C. Jones, D.J. Thompson, J. Ryue, A waveguide finite element and boundary element approach to calculating the sound radiated by railway and tram rails. J. Sound Vib 2009; 321(3-5): 813-836.

[22] Y. Zhao, X. Li, Q. Lv, H. Jiao, X. Xiao, X. Jin. Measuring, modelling and optimising an embedded rail track. Appl. Acoust 2017: 116: 70-81.

[23] P. Bouvet, N. Vincent, A. Coblentz, F. Demilly. Optimisation of resilient wheel for rolling noise control. J. Sound Vib 2000; 231: 765-777.

[24] W. Sun, D.J. Thompson, M. Toward, et al. Modelling of vibration and noise behaviour of embedded tram tracks using a wavenumber domain method. J. Sound Vib, 2020: 115446.

[25] EN 15610:2019, Railway applications – Acoustics – Rail and wheel roughness measurement related to noise generation, European Committee for Standardization, Brussels, 2019.

[26] ISO 3095:2013, Railway applications – Acoustics – Measurements of noise emitted by railbound vehicles, International Organisation for Standardization, 2013.

[27] EN 15461:2008+A1:2010: Railway applications - Noise emission - characterization of the dynamic properties of track selections for pass by noise measurements, 2010, European Committee for Standardization, Brussels.

[28] X. Zhang, D.J. Thompson, H. Jeong, M. Toward, D. Herron, C.J.C. Jones, N. Vincent, Measurements of the high frequency dynamic stiffness of railway ballast and subgrade. J. Sound Vib 2020; 468:115081.

[29] J. Ryue, S. Jang, D.J. Thompson. A wavenumber domain numerical analysis of rail noise including the surface impedance of the ground. J. Sound Vib 2018; 432: 173-191.

[30] X. Zhang, H. Jeong, D.J. Thompson, G. Squicciarini, The noise radiated by ballasted and slab tracks. Appl. Acoust 2019; 151: 193-205.

[31] X. Zhang, D.J. Thompson, E. Quaranta, G. Squicciarini, An engineering model for the prediction of the sound radiation from a railway track. J. Sound Vib 2019; 461: 114921.

[32] M.E. Delany, E.N. Bazley, Acoustical properties of fibrous absorbent materials, Appl. Acoust 1970; 3: 105–116.

[33] C.J.C. Jones, D.J. Thompson and T.P. Waters. Application of numerical models to a system of train- and track-mounted acoustic shields. Int. J. Acoust. Vib 2001; 6(4): 185-192.

[34] F. Fahy, D. Thompson (eds). Fundamentals of Sound and Vibration, 2nd edition. CRC press, Boca Raton, 2015.